BIOCHEMISTRY
including biophysical chemistry & molecular biology
Article

Biochemistry **2009,** *48,* 7251–7260 7251
DOI: 10.1021/bi900296g

Determination of the Mechanism of Action of Anti-FasL Antibody by Epitope Mapping and Homology Modeling

Victor H. Obungu,* Valentina Gelfanova, Radhakrishnan Rathnachalam, Anna Bailey, Joanne Sloan-Lancaster, and Lihua Huang

Lilly Research Laboratories, Eli Lilly and Company, Lilly Corporate Center, Indianapolis, Indiana 46285

Received February 19, 2009; Revised Manuscript Received June 30, 2009

ABSTRACT: Fas ligand (FasL) is a 40-kDa type II transmembrane protein belonging to the tumor necrosis factor (TNF) family of proteins and binds to its specific receptor, Fas, a member of the TNF receptor family. Membrane-bound FasL can be processed into a soluble form by a metalloprotease similar to that which cleaves TNFα. Elevated levels of FasL have been implicated in a wide variety of diseases ranging from cancer to inflammatory abnormalities, which could be targeted by antibody therapy. We generated a fully human high-affinity antibody against FasL that binds to and neutralizes the activity of both soluble and membrane-associated human FasL. In order to elucidate the mechanism of function of this antibody, we have mapped the region and critical residues involved in the recognition of FasL using a combination of homology modeling, immunoprecipitation, hydrogen−deuterium exchange mass spectrometry (H/DXMS), and alanine scanning site-directed mutagenesis. These studies have revealed the antibody binding site on human FasL. Furthermore, through molecular homology modeling, we have proposed a mechanism for the neutralizing activity of this antibody that involves interference with the docking of the ligand to its receptor by the antibody.

Fas ligand (FasL), also known as CD95 ligand, is a 40-kDa type II transmembrane protein consisting of 281 amino acids with a calculated molecular mass of 31759 Da. It belongs to the tumor necrosis factor (TNF)[1] family of proteins and, as such, exists as a transmembrane homotrimer (*1*, *2*). The specific receptor for FasL is Fas (CD95, Apo-1), a 45-kDa type I transmembrane protein that is a member of the TNF receptor family. Membrane-bound FasL can be processed into a soluble form by a metalloprotease similar to that which cleaves TNFα (*3*−*7*). The soluble forms of the TNF family members that have been crystallized, including TNFα (*8*), lymphotoxin α (also known as TNF*β*) (*9*), and CD40L (*10*), all share a similar compact, pear-shaped, homotrimer conformation.

FasL is predominantly expressed on activated T cells and natural killer (NK) cells, while Fas is expressed on various cell types. The Fas/FasL system plays a crucial role in modulating immune responses by inducing cellular apoptosis to maintain homeostasis, self-tolerance of lymphocytes, and immune privilege (*11*, *12*). In addition, FasL is a potent chemoattractant for neutrophils and thus also has a proinflammatory function (*13*). Genetic mutations that inactivate either FasL or Fas are associated with autoimmune lymphoproliferative syndrome, a hereditary condition characterized by the accumulation of atypical lymphocytes and by the development of autoimmune manifestations (*12*, *14*).

Tumors have evolved a variety of methods to evade the immune response. One such mechanism is the active depletion of antitumor immune cells via expression of FasL on the tumor cells. Abnormally elevated levels of FasL have been reported in leukemia and lymphomas (*3*, *15*−*20*). The Fas/Fas ligand system is also implicated in pathogenesis of many diseases, including the T cell depletion observed in HIV-infected individuals, in multiple sclerosis, in acute respiratory distress syndrome (*21*), and in acute graft-versus-host disease (*11*, *19*−*27*). The pathogenic effects of FasL can be targeted by immunotherapy involving an antagonistic antibody. While not yet demonstrated in humans, blocking of the Fas/FasL system has been shown to be therapeutic in various animal models of disease, including bacterial pneumonia (*28*), pulmonary inflammation (*29*), spinal cord injury (*30*), sepsis (*31*), and hepatitis (*32*). Such an antibody could potentially be indicated for a number of pathologies, such as autoimmune diseases and cancer.

We have generated a fully human antibody against FasL. This antibody, LA296, is an IgG4 monoclonal antibody with a binding affinity of 100 pM for soluble FasL. LA296 binds to and neutralizes the activities of both soluble and membrane-associated human and cynomolgus monkey FasL, but not that of mouse or rabbit, as determined by ELISA and BIAcore measurements. In order to further understand the epitope-binding specificity of this antibody and its mechanism of action, we have mapped critical residues involved in its recognition of FasL using a combination of homology modeling, immunoprecipitation, hydrogen−deuterium exchange mass spectrometry (H/DXMS), and alanine scanning mutagenesis. These studies have revealed the antibody binding site on human FasL. Furthermore, through molecular homology modeling, we are able to propose a mechanism for the neutralizing activity of this antibody.

*To whom correspondence should be addressed. Tel: 317-651-3962. Fax: 317-277-8200. E-mail: Obunguvi@lilly.com.

[1]Abbreviations: TNF, tumor necrosis factor; rhsFasL, recombinant human His-tagged soluble Fas ligand; rfsFasL, recombinant human Flag-tagged soluble Fas ligand; rsolFasL recombinant soluble Fas ligand; DMEM, Dulbecco's modified Eagle's medium; FCS, fetal calf serum; PCR, polymerase chain reaction; CDR, complementarity determining region; ELISA, enzyme-linked immunosorbent assay; PBS, phosphate-buffered saline; PAGE, polyacrylamide gel electrophoresis; AUC, area under the curve, MALDI, matrix-assisted laser desorption/ionization.

Published on Web 07/01/2009

MATERIALS AND METHODS

Materials. LA296 is a recombinant antibody of Eli Lilly and Co. A recombinant soluble human histidine-tagged FasL (carrier free) was obtained from R&D systems (catalog no. 126-FL-010/CF) and used for protein excision and extraction experiments. This protein (rhFasL) comprises residues 134−281 of the full length of human FasL fused at the N-terminal end to a histidine tag preceded by a single methionine residue. A Flag-tagged recombinant extracellular domain of human FasL protein (rfFasL) was purchased from Alexis (catalog no. 522-001-C010). This protein comprises residues 103−281 of the full-length human FasL fused at the N terminus to a 26 amino acid linker peptide and a Flag tag.

Cell Culture. The Jurkat cell media were comprised of RPMI 1640 (Gibco catalog no. 11875-093) supplemented 10% FBS (Gibco catalog no. 10091-148) and 50 μg/mL gentamicin (Gibco catalog no. 15750-060).

HEK 293 EBNA cells were maintained in Dulbecco's modified Eagle's medium/F-12 (3:1) supplemented with 5% fetal bovine serum, 20 mM HEPES, 2 mM L-glutamine, 50 μg/mL geneticin, and antibiotic−antimycotic mixture.

Construction, Alanine Scanning Mutagenesis, and Expression of Soluble Human FasL (*solFasL*). The soluble domain of human FasL comprising residues 133−281 was generated by PCR using a full-length FasL cDNA construct as template. The primers used in this amplification were designed to incorporate *Bam*HI and *Eco*RI sites. These restriction sites were used to clone the PCR product in-frame and downstream of a preprotrypsin leader sequence and Flag octapeptide in pFLAG CMV-1 vector (Sigma Aldrich). Alanine scanning mutants were obtained using a Quick-Change site-directed mutagenesis kit (Stratagene).

Soluble wild-type or mutant FasL cDNA was scaled up using a Maxi plasmid kit (Qiagen) as suggested by the manufacturer. The cDNA constructs thus generated were used to transiently transfect HEK 293 EBNA cells, using TransIT reagent (Mirrus) according to manufacturer's instructions. Briefly, cells were plated (5.0×10^6) onto 150 mm polylysine-coated plastic plates and grown overnight to 70−80% confluency. The medium was aspirated and replaced with 15 mL of fresh medium 0.5−1 h before transfection. The following day, medium was aspirated, cells were rinsed once with phosphate-buffered saline, and incubated for another 2−3 days in 20 mL of serum-free medium. Subsequently, the medium was collected and replaced daily for another 4−5 days. Collected media were filtered through a 0.22 um filter and concentrated using an Amicon filter with 50K MWT cutoff. The concentrates were either frozen at −20 °C or purified immediately as described below.

Purification of Wild-Type and Mutant Soluble Human FasL. SolFasL was purified by anti-Flag (M2) affinity chromatography using Cell MM2 Flag M purification kits (Sigma Aldrich). FasL was batch captured by incubating with anti-Flag resin overnight at 4 °C. The following day the mixture was centrifuged on a bench centrifuge, and the resin was collected, washed twice with wash buffer, and packed into a chromatography column. The column was washed with 10 column volumes of wash buffer or until the OD_{280} of flow through eluate was below 0.05. FasL was eluted from the column using elution buffer (0.1 M glycine, pH 3.5) into tubes containing 1 mL of Tris buffer, pH 8.0. Eluates were pooled, concentrated by Amicon filters, and buffer exchanged twice in phosphate-buffered saline (PBS) buffer, pH 7.4. This soluble FasL largely migrated at 30 kDa in a reduced SDS−PAGE gel despite a theoretical mass of 18 kDa, likely as a result of glycosylation.

FasL-Mediated Cell Death Assay in Jurkat Cells. In order to run a cell death assay, a 4× FasL/enhancer medium was prepared. This medium was made up by incubating Jurkat cell media, 200 ng/mL FasL, and 4.0 μg/mL anti-Flag M2 mAb (Sigma catalog no. F-3165) (enhancer) for 1 h at room temperature to allow for binding of enhancer to FasL and "multimerization" to occur. In the meantime, 4× serial dilutions of samples (FasL inhibitors) and controls were made as needed. 4× FasL/enhancer media (25 μL/well) or controls were aliquoted into the 96-well plate. At the same time, 25 μL/well of samples or controls was similarly aliquoted into the 96-well plate. The plate was incubated for 1 h to allow binding of samples to enhanced FasL. A total of 1000000 Jurkat cells/mL of solution were aliquoted at 50 μL/well and incubated for 3 h at 37 °C in a 5% CO_2 incubator. Ten microliters of WST-1 cell proliferation reagent (Roche catalog no. 1 644 807) was subsequently aliquoted into each well and the plate incubated for approximately 18 h (overnight) at 37 °C in a 5% CO_2 incubator. The following day the plate was read on a Molecular Devices plate reader at an optimal wavelength of 450 nm.

Epitope Extraction. RhFasL (R&D, carrier-free) was reconstituted in 100 mM NH_4HCO_3 buffer, pH 8, and digested with trypsin at 37 °C for 6 h. LA296 was biotinylated with NHS-LC-biotin (Pierce) according to manufacturer's protocol. Dynalbeads M-280 streptavidin (100 μL) was incubated with 5 μg of biotinylated LA296 for 6 h at room temperature, and unbound antibody was removed by washing the beads with PBS. One microgram of the FasL tryptic digest was diluted in PBS/0.1% BSA buffer and added to the washed beads. After overnight incubation at 4 °C, beads were washed three times with PBS and twice with 100 mM ammonium bicarbonate buffer, pH 8. Bound peptides were eluted from the beads in 10% formic acid, desalted with ZipTip C18, and spotted onto MALDI targets with an equal volume of saturated α-cyano-4-hydroxycinnamic acid solution added.

Epitope Excision. A mixture of LA296 and rhFasL in PBS/0.1% BSA was incubated for 6 h at 4 °C. Antibody−protein complexes were captured with Protein A−Sepharose beads (Amersham) and subjected to the digestion with trypsin. Bound peptides were eluted from the beads and analyzed as described above.

In a separate experiment, LA296, FasL, and a mixture of LA296 and FasL were incubated in PBS overnight at 4 °C and then digested with trypsin (6 h at 37 °C). Tryptic digests were desalted with ZipTip C18, and peptides were analyzed by MALDI TOF.

MALDI-Mass Spectrometry. All spectra were acquired with a 4700 MALDI-Tof-Tof mass spectrometer (PerSeptive Biosystems, Framingham, MA) as described (*33*).

Hydrogen−Deuterium Exchange Mass Spectrometry (*H/DXMS*). Flag-tagged soluble human FasL (Alexis) was used in this analysis. FasL−LA296 complexes were prepared as follows: 10 μg of FasL (10 μL) solution was transferred to a 500 μL plastic vial. Then either 5 μL of 1× PBS (10 mM sodium phosphate, 150 mM NaCl, pH 7.4) or 5 μL (50 μg) of LA296 was added, yielding an approximate molar ratio (FasL/LA296) of 1:1.5. Twenty microliters of 1× PBS was added into each vial, and each solution was then treated with 1 μL of 1 unit/mL neuraminidase solution (Roche Diagnostics) at 37 °C for 90 min.

Five microliters of free FasL or the FasL−LA296 complex was mixed with 20 μL of 100% D_2O, resulting in 80% D_2O in the final sample. The solution was incubated at ambient temperature for 10 min. The exchange was quenched, and the sample was digested by adding 2 μL of 2 mg/mL pepsin (Sigma) and 20 μL of 0.15% formic acid aqueous solution and incubating at ambient temperature for 30 s. The digest was immediately injected onto a C18 reversed-phase column, manually.

A Waters 2795 HPLC and Micromass LCT premier mass spectrometer were used for all analyses. The HPLC stream from the HPLC pump was connected via metal tubing (approximately 1 mL) to the manual injector and to a Zorbax C18 column (2.1 × 50 mm) and then to the mass spectrometer. The metal tubing, injector loop, and column were continuously submerged in ice water. The column was equilibrated with 99% A (0.15% formic acid in aqueous solution) and 1% B (0.12% formic acid in acetonitrile) at flow rate of 0.2 mL/min. A gradient elution was performed from 1% to 15% B over 2 min, to 40% B over 13 min, to 90% B over 1 min with 2.5 min hold, and then returned to the initial conditions in 2.5 min. The mass spectrometry was performed with the following settings: a capillary voltage of 3.0 kV, a cone voltage of 80 V, aperture 1 voltage of 15, a mass range of 300−3500, a desolvation temperature of 300 °C, and a desolvation gas flow of 700 L/h. The mass spectrum of each peptic fragment of FasL was obtained after H/D exchange with or without LA296 present. The average mass of each peptide was calculated according to the isotopic distribution of the most intense ion peak (*34*, *35*).

Three-Dimensional Homology Modeling of FasL and the Fas−FasL Complex. In order to identify structures with folds compatible with the human FasL sequence, the SEQFOLD/HOMOLOGY module (Insight, Accelrys Software Inc., San Diego, CA) was used, with the secondary structure prediction by DSC (*26*). From this analysis, TNF-α and TNF-α receptor (Brookhaven Protein Data Bank entries 2TNF and 1TNR), respectively, had the highest compatibility scores with FasL and the Fas−FasL complex. The homology models of FasL (and Fas−FasL) were therefore generated using crystallographic structures of 2TNF and 1TNR as templates (*36*, *37*). Homology modeling of FasL was built by first identifying conserved regions in the two structures during which process an rms limit of 0.75 Å was used. The sequences were aligned and coordinates of the conserved regions in the target sequence modeled using the corresponding regions in the templates. The final model was refined by initially keeping the backbone atoms fixed followed by having all of them restrained. The trimeric model was built by using the 3D trimeric structure of 2TNF and refined by initially keeping the backbone atoms fixed and then further by using a harmonic restraint for all atoms. The quality of the model was assessed by calculating the compatibility score (Profile-3D module; Insight Software Inc., San Diego, CA). The score was 53/62 (53 is the score for the actual model, and 62 is the expected score for a protein of the same length as the model protein) for the monomeric model and 58/64 for the corresponding domain of 2TNF. For the trimeric model, the score was 202/188, whereas for 2TNF it was 210/202. These scores suggested that the model was of high enough quality to allow reliable interpretation of the data.

Determination of Binding Affinity and Kinetics Using Surface Plasmon Resonance (*BIAcore*). Binding affinity and kinetics of soluble wild-type FasL and its analogues were measured using surface plasmon resonance with a BIAcore 2000 instrument containing a CM5 sensor chip. Protein A was immobilized onto flow cells 1 and 2 using amine-coupling chemistry. Flow cells were activated for 7 min with a 1:1 mixture of 0.1 M *N*-hydroxysuccinimide and 0.1 M 3-(*N*,*N*-dimethylamino)propyl-*N*-ethylcarbodiimide at a flow rate of 5 μL/min. Protein A (35 μg/mL in 10 mM sodium acetate at pH 4.5) was injected over both flow cells for 2−3 min at 5 μL/min, which resulted in a surface density of 700−800 response units (RU). Surfaces were blocked with a 7 min injection of 1 M ethanolamine−HCl at pH 8.5. To ensure complete removal of any noncovalently bound protein A, 15 μL of 10 mM glycine at pH 1.5 was injected twice. Unless stated otherwise in the text, the running buffer used for kinetic experiments contained 10 mM HEPES at pH 7.4, 150 mM NaCl, 0.005% P20, and 3 mM EDTA (HBS-EP), purchased from BIAcore. All experiments were performed at 25 °C. Each analysis cycle consisted of (i) the capture of 140−200 RU of antibody by injection of 10−20 μL of approximately 2 μg/mL antibody over flow cell 2, (ii) a 2 min stabilization time, (iii) a 250 μL injection of sFasL analogues (concentration range of 100−0.78125 nM in 2-fold dilution increments) over flow cells 1 and 2, using flow cell 1 as the reference flow cell, (iv) a 10 min dissociation (buffer flow), (v) the regeneration of protein A surface with a 30 s injection of 10 mM glycine at pH 1.5 at 20 μL/min, (vi) a 45 s blank injection of running buffer at 20 μL/min, and (vii) a 2 min stabilization time before the start of the next cycle. The signal was monitored as flow cell 2 minus flow cell 1. Samples and a buffer blank were injected in triplicate. The data from buffer blank (0 nM concentration) was subtracted from all of the sample runs. This method is referred to as double referencing, which should correct for any dissociation of LA296 from protein A during the run; however, it should be noted that during the time scale of the binding experiments no dissociation of LA296 from protein A was observed. The normalized data were then simultaneously fit to a 1:1 binding with mass transport model using global data analysis in BIAevaluation 3.1 software to obtain k_{on} and k_{off} parameters. K_d was calculated as a ratio of K_{off}/K_{on}.

RESULTS AND DISCUSSION

LA296 Binds to FasL by ELISA and Inhibits FasL-Mediated Apoptosis in Jurkat Cells. LA296 was initially tested and shown to bind human FasL but not mouse FasL in an ELISA (data not shown). In order to determine whether LA296 neutralized the activity of FasL, an *in vitro* cell death assay using Jurkat T cells and rfFasL was done. Death of Jurkat T cells was initiated by incubation with anti-Flag M2 antibody cross-linked FasL. Addition of two independently prepared lots of LA296 inhibited FasL-mediated cell death in a dose-dependent manner (Figure 1), indicating that LA296 is a potent inhibitor of FasL-mediated Jurkat cell death with an IC_{50} of about 0.2 nM.

LA296 Binds to both Monomeric and Trimeric Forms of FasL. In order to determine the form of FasL to which LA296 specifically binds, we used immunoprecipitation to establish whether the antibody binds to monomeric FasL or specifically recognizes the trimeric form. FasL was obtained from two vendors, Alexis and R&D systems. While soluble FasL from Alexis was shown by MALDI-MS and nonreducing SDS−PAGE to be largely trimeric, that from R&D systems was predominantly monomeric (data not shown). Recombinant human FasL from the two sources were individually incubated with LA296−biotin−streptavidin magnetic beads or with

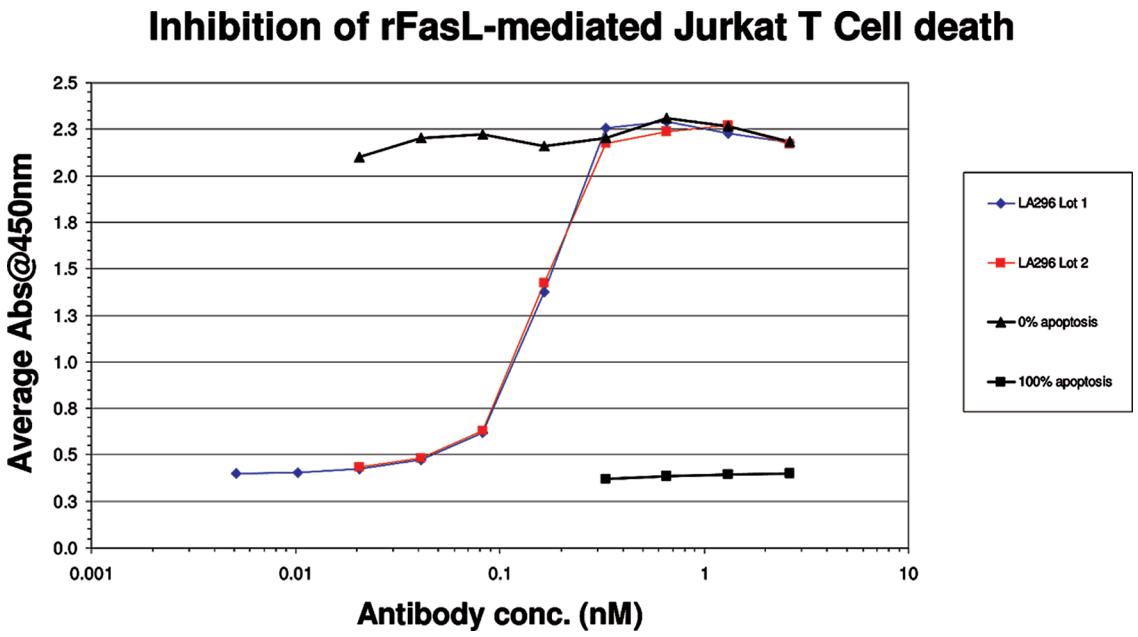

FIGURE 1: RfFasL-induced apoptosis of a Fas+ Jurkat cell line treated with either media alone (0% apoptosis), rFasL alone (100% apoptosis), or rFasL preincubated with various concentrations of anti-FasL mAb LA296. The data show a decrease in cell death as the concentration of LA296 increases, suggesting that LA296 binds to rFasL and blocks its cell killing activity.

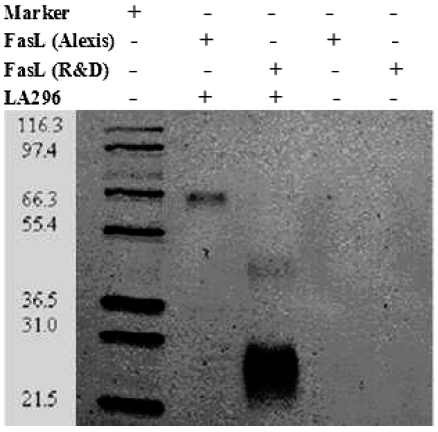

FIGURE 2: Immunoprecipitation of FasL. FasL (3 μg) from Alexis (lanes 2 and 4) or R&D (lanes 3 and 5) was precipitated with 100 μL of streptavidin beads with (lanes 2 and 3) or without (lanes 4 and 5) immobilized biotinylated LA296. Proteins were separated under nonreducing conditions. Line 1 is MARK 12 protein standards.

control beads. Bound FasL was eluted from beads and separated on SDS−PAGE under nonreducing conditions. As shown in Figure 2, FasL trimers (Alexis) and FasL monomers and dimers (R&D) were specifically immunoprecipitated with LA296 antibody-coated beads. This experiment, together with the observation that LA296 binding to FasL could be detected by Western blot after separation in a reducing SDS−PAGE gel (data not shown), suggests that the antibody's binding site resides in a FasL monomer.

LA296 Does Not Bind FasL Tryptic Fragment Peptides. Histidine-tagged monomeric recombinant human FasL (rhFasL) was digested with trypsin. The resulting tryptic digest mixture was directly analyzed by MALDI-MS (*33*) or diluted with a PBS/0.1% BSA buffer and incubated with biotinylated LA296 bound to streptavidin magnetic beads or to control beads. Peptides bound to the beads were eluted and eluates analyzed by MALDI-MS and SDS−PAGE. A 21-kDa band was detected by SDS−PAGE, and

Table 1: Peptides Identified in 6 h Tryptic Digest of rhFasL[a]

peptide ID	corresponding full-length FasL peptide	amino acid sequence
1	Tag-140	MHHHHHHPSPPPEK
2	Tag-141	MHHHHHHPSPPPEKK
3	Tag-145	MHHHHHHPSPPPEKKELRK
4	145−152	KVAHLTGK
5	145−156	KVAHLTGKSNSR
6	157−175	SMPLEWEDTYGIVLLSGVK
7	176−194	YKKGGLVINETGLYFVYSK
8	178−194	KGGLVINETGLYFVYSK
9	179−194	GGLVINETGLYFVYSK
10	195−210	VYFRGQSCNNLPLSHK
11	199−217	GQSCNNLPLSHKVYMRNSK
12	211−228	VYMRNSKYPQDLVMMEGK
13	215−228	NSKYPQDLVMMEGK
14	218−228	YPQDLVMMEGK
15	229−241	MMSYCTTGQMWAR

[a] The following is the sequence of rhFasL used in these studies (the tag is underlined): MHHHHHHPSPPPEKKELRKVAHLTGKSNSRSMPLEWEDTYGIVLLSGVKYKKGGLVINETGLYFVYSKVYFRGQSCNNLPLSHKVYMRNSKYPQDLVMMEGKMMSYCTTGQMWARSSYLGAVFNLTSADHLYVNVSELSLVNFEESQTFFGLYKL.

a number of FasL peptides were identified by MALDI-MS (Table 1). However, no peptides specific for rhFasL were detected in the eluates from LA296 beads in MALDI mass spectra or by SDS−PAGE, indicating that none of the peptides bound to the LA296-coated beads. These observations suggested that the LA296 binding region of FasL might be assuming some local conformational fold that is disrupted during trypsin digestion, thereby preventing binding of the peptides to the beads.

LA296 Protects FasL from Being Cleaved with Trypsin. In an epitope excision experiment, LA296 was incubated with or without FasL in PBS/0.1% BSA for 6 h at 4 °C. Antibody or antibody−antigen complexes were captured with protein A−Sepharose beads (Amersham) and then digested with trypsin. Bound peptides were eluted from the beads, desalted, and

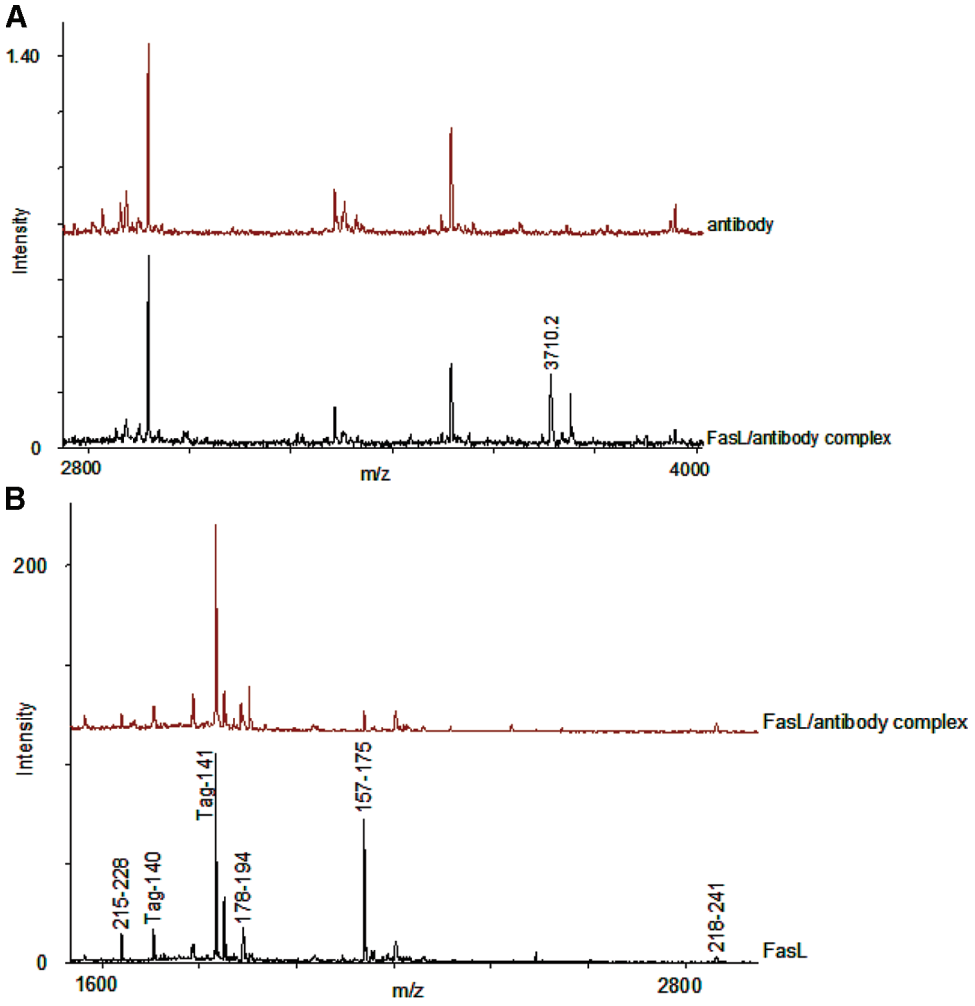

FIGURE 3: (A) Epitope excision. LA296 or the LA296−FasL complex immobilized on protein A−Sepharose beads was digested with trypsin. Bound peptides were eluted from beads, desalted, and analyzed by MALDI-MS. The peptide with m/z 3710.2 was found in the eluate from the LA296/FasL sample but not from the LA296 sample. (B) LA296 protects FasL from being cleaved with trypsin at the arginine 156 position. LA296 or the LA296−FasL complex was digested with trypsin. Peptides were desalted and analyzed by MALDI. Tryptic peptide 157−175 is less abundant in the LA296−FasL digest.

analyzed by MALDI. A peptide with m/z 3710.2 was found in the eluate from the LA296/FasL sample but not in the LA296 sample, suggesting it could represent a FasL-derived peptide (Figure 3A). In a separate experiment, LA296 alone, FasL alone, or a mixture of the two was incubated in PBS overnight at 4 °C and then digested with trypsin (6 h at 37 °C). Tryptic digests were desalted with ZipTip C18 and peptides analyzed by MALDI-MS. Peptides that were found in the free FasL or LA296-FasL samples, but not in the LA296 control sample, were assigned as FasL peptides (Tables 2 and 3). The identity of peptides 157−175, 178−194, 215−228, and 218−228 (i.e., peptides 6, 8, 13, and 14, respectively) was also confirmed by LC/MS/MS analysis of the same digests (data not shown). As shown in Figure 3B, similar FasL peptides were recovered from both samples. However, in the presence of LA296, much less of peptide 157−175 (peptide 6) was detected (Table 3), suggesting that the antibody binding epitope may be present within this peptide. It is worth noting that this region is flanked by an arginine residue at position 156 which appears to be protected from trypsin digestion in the presence of LA296.

Confirmation and Further Identification of the Region of FasL That Binds LA296 by H/DXMS Analysis. To further confirm the identity of the residues in FasL involved in LA296 binding, we employed H/DXMS (*34*, *35*) to identify regions of soluble FasL that are protected from exchange with deuterated water (D_2O) upon binding to LA296. The exchange rate of backbone amide hydrogen in a protein−protein complex is highly dependent on whether the amide group participates directly in binding or is otherwise situated at the interface region. Upon binding LA296, the FasL amide groups participating in this interaction should have a slower hydrogen to deuterium exchange rate compared to that of the same residues in free FasL. When one hydrogen is exchanged for one deuterium, the mass will be increased one unit. (Note: each amino acid residue in a peptide or protein contains one amide hydrogen except Pro and the N-terminal residue; H/DXMS only measures amide

Table 2: Tryptic Digest Peptides Assigned to rhFasL

peptide ID	corresponding full-length FasL peptide	amino acid sequence
1	Tag-140	MHHHHHHPSPPPEK
2	Tag-141	MHHHHHHPSPPPEKK
6	157−175	SMPLEWEDTYGIVLLSGVK
8	178−194	KGGLVINETGLYFVYSK
13	215−228	NSKYPQDLVMMEGK
14	218−228	YPQDLVMMEGK
16	218−241	YPQDLVMMEGKMMSYCTT GQMWAR

Table 3: Effect of LA296 on the Relative Amounts of FasL Tryptic Fragments

peptide ID	corresponding full-length FasL peptide	AUC for peptide in FasL	AUC for peptide in FasL/LA296	ratio between samples
1	Tag-140	44445	31697	1.22
2	Tag-141	430830	352027	1.40
6	157−175	2031128	31612	64.25
8	178−194	35376	27317	1.30
13	215−228	39302	28517	1.38
16	218−241	9276	13551	0.68

Table 4: Effects of LA296 on Hydrogen−Deuterium Exchange in FasL Determined by Masses of Peptic Digest Fragments[a]

peptide ID	corresponding full-length FasL peptide	Δmass (n = 3)	SD
A	tag+ linker	0.2	0.3
B	linker−121	1.4	0.1
C	105−114	0.0	0.1
D	115−127	0.2	0.3
E	122−127	0.1	0.1
F	128−167	−4.6	0.7
G	128−161	−0.9	0.3
H	162−167	−1.2	0.2
I	168−281	−1.0	2.9

[a] Δmass = peptide fragment mass (FasL in FasL/LA296) − peptide fragment mass (free FasL). Sequences here are for soluble FasL fused to Flag octapeptide at the N terminus.

hydrogen exchange.) Thus, comparing peptide fragment mass between proteolytic digests of FasL only and the FasL−LA296 complex allows for identification of the peptides that have different exchange rates. These peptides are either within the antibody binding site, or they could be at a distal site but have an induced conformational change upon antibody binding.

The first step in mapping the LA296 epitope in FasL by H/DXMS was to assign peptic digest fragment peptides for FasL in H_2O. The next step in this procedure was to obtain the mass of each peptic digest peptide fragment of FasL for the free and LA296-complexed FasL after H/D exchange and then calculate the mass difference between them. The mass differences obtained by H/DXMS for the peptic digest fragment peptides between the free and complexed FasL are listed in Table 4.

Three FasL fragment peptides, 128−167, 128−161, and 162−167, showed significant negative mass differences between the FasL−LA296 mixture and free FasL after hydrogen/deuterium exchange (Table 4). The sum of mass differences for peptides 128−161 and 162−167 is very different from that of 128−167, suggesting amino acid residues around 161 and 162 are protected and therefore reside within the binding site. This is partly because pepsin cleavage between Glu-161 and Trp-162 eliminates one backbone amide bond (i.e., eliminates one amide hydrogen). Furthermore, hydrogens near N termini of a peptide have faster back-exchange rates than the internal amide hydrogens. Thus, the amide hydrogens of amino acid residues around Glu-161 and Trp-162 were largely exchanged with deuterium for the free FasL and retained for the LA296/FasL complex, but pepsin cleavage between Glu-161 and Trp-162 caused rapid back-exchange near the cleavage site, thereby reducing the apparent effect of LA296 binding on hydrogen−deuterium exchange in this region of the molecule. For the glycopeptide 168−281, the mass difference was −1, which was not significant, as evidenced by the large standard deviation of (±2.9), likely mainly due to its size and heterogeneous N-glycosylation. Note that, during the peptic digest and LC/MS analysis, back-exchange could occur at up to 50% for very small peptides on the basis of control experiments (data not shown). Thus, if the back-exchange could be completely prevented, the mass difference detected would be 2−3 Da for peptides 128−161 and 162−167. As mentioned previously, except for Pro and N-terminal residues, each amino acid residue has a single backbone amide hydrogen; therefore, after hydrogen−deuterium exchange, the peptide or protein mass increases 1 Da per backbone amide hydrogen. Hence, a 2 or 3 Da difference means that two to three amino acid residues in those peptides were protected from exchange by the antibody; i.e., they were involved in binding (belong to the epitope) or they were in contact with non-CDR regions of the antibody. The results are consistent with those obtained from epitope extraction and excision experiments.

Interestingly, peptide B (linker−121) showed a positive mass difference between the complexed and free FasL; i.e., the exchange rate of this peptide is faster for the complexed FasL than the free FasL. Therefore, this region of the protein is likely not part of the binding site. A plausible explanation for these observations is that, after LA296 binds FasL, the conformation of FasL may be changed in such a way that this region of the molecule becomes more solvent exposed.

Analysis of the Homology Model of Human FasL. Homology modeling of FasL was undertaken in order to predict the site where LA296 binds human FasL. This modeling took into consideration the fact that the antibody bound to both monomeric and trimeric forms of human FasL, but not to those of mouse or rabbit. Thus, we reasoned that the residues within this site should be different between human and the mouse or rabbit sequences and should also be exposed in order for the antibody to bind.

Analysis of the homology model of FasL for surface-exposed patches of residues together with sequence comparison of human with mouse and rabbit sequences yielded two regions which could be antibody binding sites. The critical residue within the first potential epitope was methionine 158 which lies within the N-terminal segment of the peptide, N154−W162 (Figure 4). This residue satisfied the criteria that it should vary between human and mouse and the rabbit sequences as well as being exposed not only in the monomer but also upon trimer formation. Moreover, it lies in a flexible region without having strong secondary structural features. The other candidate epitope was that around leucine 205 comprising the peptide C202−S208. However, this region did not exhibit the same degree of flexibility or exposure as the site around methionine 158 and was therefore considered a less likely possibility. The two residues M158 and L205 alongside others identified by epitope excision and hydrogen−deuterium exchange were subjected to alanine scanning mutagenesis. These two possible epitopes are shown in Figure 4.

Analysis of LA296 Binding to FasL by BIAcore Analysis. LA296 was captured on the surface of a BIAcore CM4 chip through immobilized protein A. Binding of human FasL to the antibody was monitored as a function of FasL concentrations. Figure 5 shows an overlay of the fitted sensorgrams and data for successive injections of 11 FasL concentrations. LA296 was found to bind FasL with a K_d of less than 100 pM, with a k_{on} of 5×10^4 M^{-1} s^{-1} and a k_{off} of $< 1 \times 10^{-5}$ s^{-1}. LA296 bound the three versions of wild-type FasL with identical affinities (data not shown).

Alanine Scanning Mutagenesis and Analysis of Binding by BIAcore. In order to confirm the identity of the amino acid residues of FasL involved in the binding of LA296, we performed alanine scanning mutagenesis of the residues in the regions of the protein identified by epitope excision, hydrogen−deuterium exchange, and homology modeling analyses. The following residues were changed by site-directed mutagenesis to alanine: S157, M158, P159, L160, E161, W162, E163, D164, T165, Y166, and L205. All mutants (Flag tagged) were expressed transiently in HEK 293 EBNA cells and purified to homogeneity by affinity chromatography with the exception of the E163A mutant which failed to express.

Wild-type and FasL mutants were next tested by BIAcore for binding by LA296. As before, LA296 was captured on a BIAcore chip through immobilized protein A. Binding of wild-type and mutant human FasL to LA296 was monitored by comparing binding profiles (k_{on} and k_{off}) of wild-type and alanine scanning mutants of FasL as well as RANKL, a TNF family member as a negative control. As shown in Figure 6 and summarized in Table 5, LA296 could not bind to either the L160A or W162A mutants. This suggests that these two residues play a central role in the binding of the antibody to FasL. On the other hand, some mutants were bound with dramatically altered kinetics. Those with slower k_{on} and faster k_{off} rates included M158A, P159A, E161, and Y166A, with the latter showing the fastest dissociation rate of all the mutants. Detailed kinetic binding analysis was further done for E161A and Y166A. This analysis revealed a 50- and 6000-fold reduction in binding affinity (K_d) for E161A and Y166A, respectively (Table 5). This suggests that they are part of the antibody binding epitope and may play a supportive role during the binding of LA296 to FasL. As expected, the control protein, RANKL, was not bound by LA296 (Figure 6B) while S157A, D164A, T165A, and L205A mutants bound LA296 with apparently identical association and dissociation rates as the wild type (Figure 6).

FIGURE 4: A ribbon diagram of the monomer of FasL generated via homology modeling of the crystal structure of TNF-α. The β sheet is in yellow while the predicted epitopes are shown in red and purple. The loops are shown in green.

In summary, we have generated LA296, an antibody that neutralizes FasL biological activity. In order to understand its mechanism of action, we have determined its epitope in soluble FasL by four complementary approaches: epitope extraction, epitope excision, hydrogen−deuterium exchange, and homology modeling. These were followed by BIAcore binding and kinetic analysis of site-directed mutants. While epitope extraction was unsuccessful, epitope excision showed that LA296 could protect FasL from being cleaved by trypsin at arginine 156 and lysine 175, since mass spectroscopic analysis of the tryptic digest revealed a dramatic reduction of the 157−175 fragment relative to the other FasL fragments in the presence of LA296. The results indicated that this portion of FasL comprised the antibody binding site. Additional analysis using hydrogen−deuterium exchange and homology modeling narrowed the location of the antibody epitope further to amino acids 158−166. Site-directed mutants were generated for selected residues within this loop and their ability to be bound by LA296 studied by BIAcore. In addition, other flanking residues were mutated to determine whether they also contributed to the binding interaction. LA296 bound wild-type FasL with high affinity with K_d in the sub-nanomolar range. This high affinity was driven mainly by a slow off rate of the antibody (*37*, *38*). The BIAcore data fit well to a 1:1 binding stochiometry with the mass transport kinetic model. It is

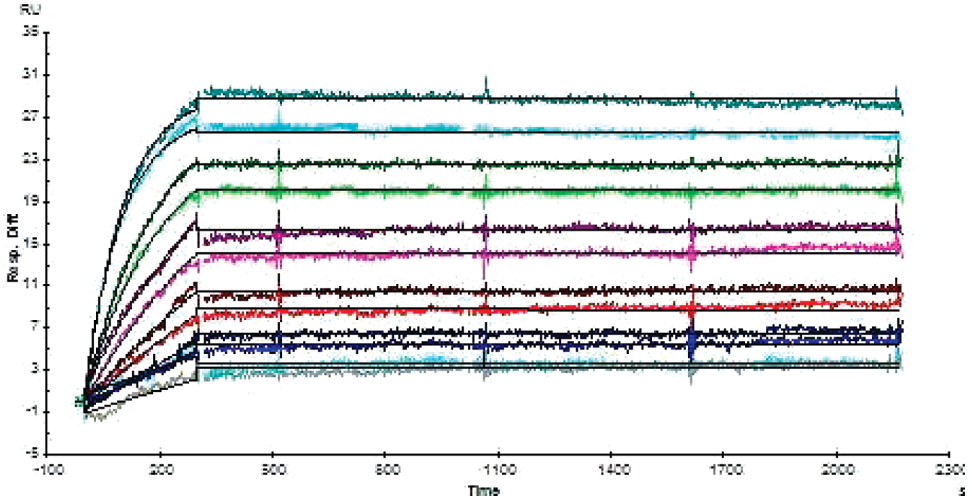

FIGURE 5: BIAcore sensorgram data and global analysis of human FasL binding to LA296. FasL (100, 50, 25, 12.5, 6.25, 3.125, 1.5625, 0.78125, 0.390625, 0.1953125, and 0.0.09765625 nM) was injected over a control surface (no LA296) and a surface containing LA296 with the dissociation monitored for 20 min. The data were collected in duplicate for each FasL concentration. The association and dissociation phases were globally fit to a 1:1 mass transport limited model. The fit of the data is shown as a solid line.

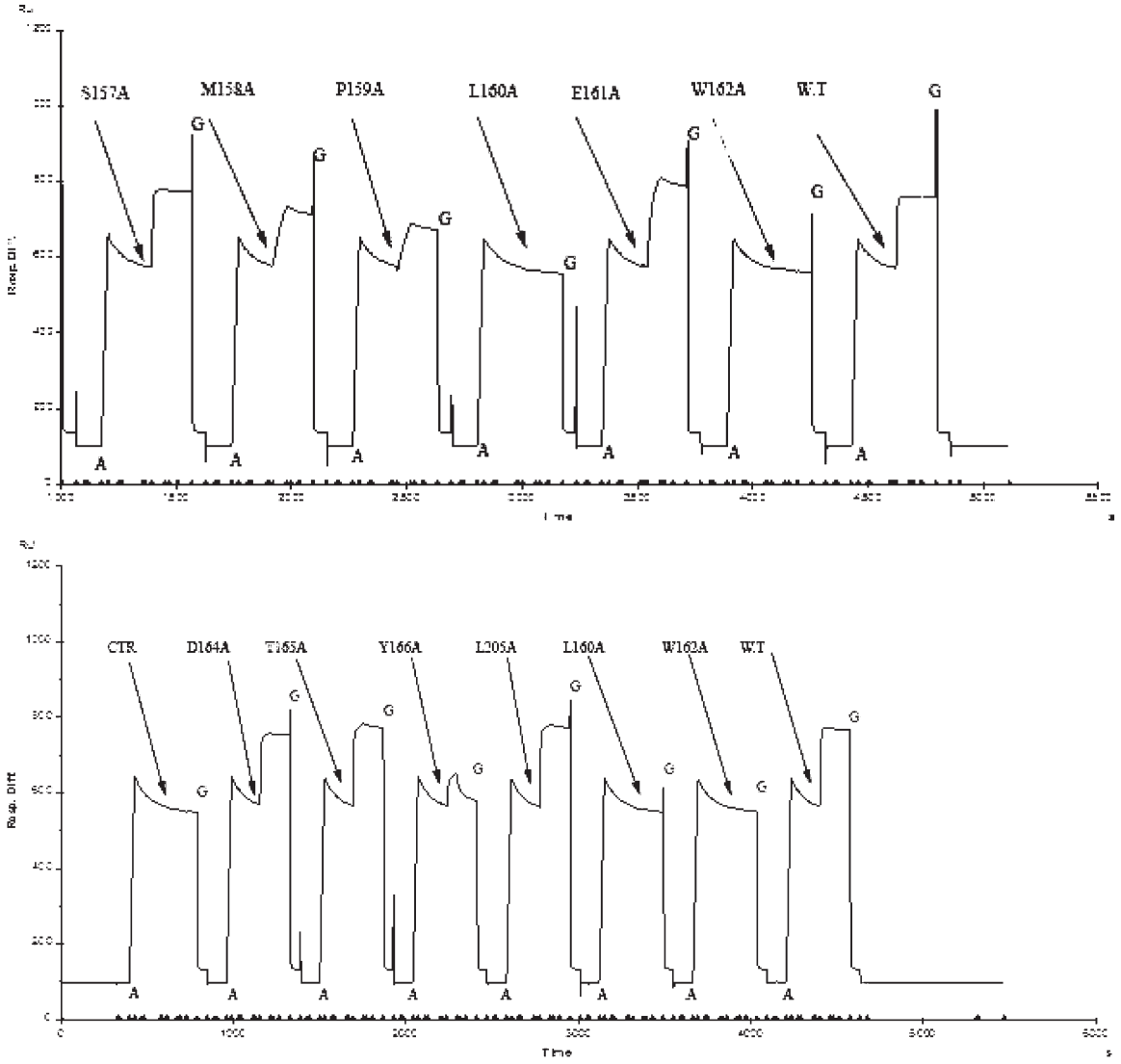

FIGURE 6: BIAcore sensorgram data of wild-type and mutant human FasL binding to LA296. (A) Alanine mutants at positions 157−162 and wt. (B) Negative control RANKL; alanine mutants at positions 160 (repeat), 162 (repeat), 164−166, and 205; and wt. FasL (100 nM) was injected over a control surface (no LA296) and a surface containing LA296 with the dissociation monitored for 5 min. The antibody capture (A) as well as FasL association (arrow) and dissociation profiles is shown. The surface was regenerated by 1 mM glycine as shown (G).

Table 5: Summary of Binding of LA296 to Alanine Scanning Mutants and Kinetic Analysis for Selected Mutants As Determined by BIAcore[a]

FasL protein	LA296 binding[b]	K_{on} (M^{-1} s^{-1})	K_{off} (s^{-1})	K_d (affinity) (nM)
wild type	++++	**5×10^4**	**$< 1 \times 10^{-5}$**	**< 0.100**
S157A	++++	ND	ND	ND
M158A	++	ND	ND	ND
P159A	++	ND	ND	ND
L160A	−	ND	ND	ND
E161A	++	**1.7×10^5**	**8.4×10^{-4}**	**4.85**
W162A	−	ND	ND	ND
D164A	++++	ND	ND	ND
T165A	++++	ND	ND	ND
Y166A	+	**4.2×10^5**	**2.1×10^{-2}**	**507**
L205A	++++	ND	ND	ND

[a] Experiments were performed at 25 °C in 10 mM HEPES at pH 7.4, 150 mM NaCl, 0.005% P20, and 3 mM EDTA (HBS-EP). Reported kinetic values are the mean ± SEM for three independent experiments that were each fit globally. [b] (++++) is binding profile similar to the wild type; (−) indicates no binding; ND, not determined.

worth noting that, despite the stoichiometry, avidity events with the bivalent antibody IgG4 could not be entirely ruled out. However, due to difficulty in generating Fabs by papain digestion, Fab fragments were not used in the present analysis.

We next evaluated binding profiles of LA296 to the site-directed mutants. Mutation of M158 to alanine showed a decreased rate of association but an increased rate of dissociation, suggesting some role in mediating the binding of the antibody to FasL, consistent with the prediction that this residue lies within or in close proximity to the antibody epitope. However, when L205 was mutated to alanine, there was no change in either k_{on} or k_{off}, indicating that this residue was not involved in binding of LA296 to FasL. Similarly, S157A, D164A, and T165A mutants bound LA296 with apparently identical association and dissociation rates as the wild type, suggesting that these residues are not critical for antibody binding to the FasL. However, P159A, E161A, and Y166A exhibited slower k_{on} and faster k_{off}, with the latter showing the fastest dissociation rate of any of the mutants studied. Detailed kinetic binding analysis was performed for E161A and Y166A, revealing about 50- and 6000-fold reductions, respectively, in binding affinity (K_d) (Table 5). This suggests that these residues are part of the antibody binding epitope and may play a supportive role in binding of LA296 to

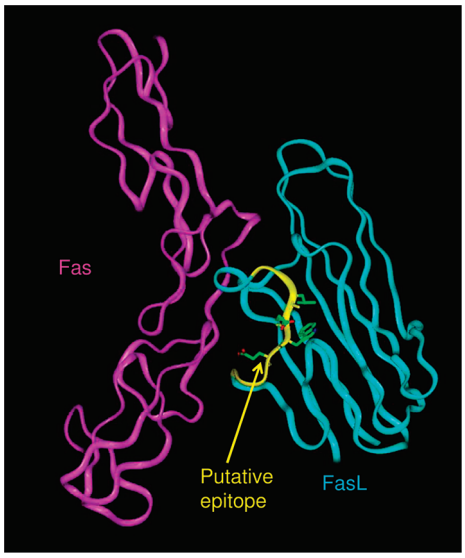

FIGURE 7: Monomeric model of Fas/FasL. The putative LA296 epitope is shown in yellow.

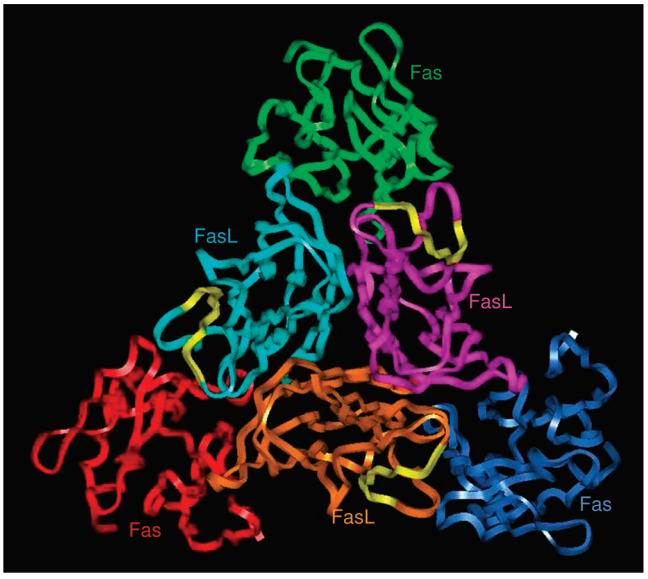

FIGURE 8: Trimer model of Fas/FasL. The putative LA296 epitope is shown in yellow.

FasL. Two mutants, L160A and W162A, completely abrogated binding of the antibody to FasL, showing that they play the most critical role in the antibody−antigen interaction. Taken together, the data suggest that residues 158−166, which are predicted by homology modeling to form a flexible loop, comprise the core of the LA296 binding epitope. Amino acids L160 and W162 play a critical role and are perhaps the nexus of this local fold that is recognized by the antibody. It is also likely that the amino acid E163 plays a key structural role in this loop as indicated by the failure of the E163A mutant to express at all in mammalian cells. Thus, residues L160, E161, W162, and E163 likely form the central core of the LA296 antibody binding site in FasL (Figure 7). This epitope is different from that reported for other FasL antibodies, NOK-1, -2, and -3 (*40*).

In order to understand why antibody binding to this loop might lead to neutralization of FasL activity as shown by inhibition of FasL-mediated Jurkat cell death, we performed computer modeling of FasL and its receptor, based on the crystal structure of the TNF-α/TNF receptor complex (*36*). Our modeling analysis of receptor ligand interaction shows that the loop identified in our studies as important for antibody binding lies in close proximity to the FasL−Fas interface (Figure 7). This close proximity is observed in both the monomeric (Figure 7) and trimeric forms of the Fas−FasL complex (Figure 8). Since the antibody is bulky, its binding to the peptide loop, identified here as the epitope, would prevent optimal receptor interaction via steric hindrance rather than directly blocking access to the residues of FasL predicted in earlier reports to participate in receptor binding (*11*, *20*, *41*). This abrogation of optimal ligand docking onto the receptor would therefore lead to loss of FasL signaling activity.

In conclusion, we have generated an antagonistic antibody to FasL and elucidated its mechanism of action by using epitope mapping. This neutralizing anti-human FasL antibody could be used as a therapeutic agent in multiple diseases that result from excessive signaling through Fas upon binding of its ligand.

ACKNOWLEDGMENT

We thank Drs. Radmila Micanovic and Wayne Kohn for thoroughly proofreading the manuscript.

REFERENCES

1. Nagata, S. (1997) Apoptosis by death factor. *Cell 88*, 355–365.
2. Smith, C. A., Farrah, T., and Goodwin, R. G. (1994) The TNF receptor superfamily of cellular and viral proteins: activation, costimulation, and death. *Cell 76*, 959–962.
3. Tanaka, M., Suda, T., Haze, K., Nakamura, N., Sato, K., Kimura, F., Motoyoshi, K., Mizuki, M., Tagawa, S., Ohga, S., Hatake, K., Drummond, A. H., and Nagata, S. (1996) Fas ligand in human serum. *Nat. Med. 2*, 317–322.
4. Gearing, A. J. H., Beckett, P., Christodoulou, M., Churchill, M., Clements, J., Davidson, A. H., Drummond, A. H., Galloway, W. A., Gilbert, R., Gordon, J. L., Leber, T. M., Mangan, M., Miller, K., Nayee, P., Owen, K., Patel, S., Thomas, W., Wells, G., Wood, L. M., and Woolley, K. (1994) Processing of tumour necrosis factor-alpha precursor by metalloproteinases. *Nature 370*, 555–557.
5. Kayagaki, N., Kawasaki, A., Ebata, T., Ohmoto, H., Ikeda, S., Inoue, S., Yoshino, K., Okumura, K., and Yagita, H. (1995) Metalloproteinase-mediated release of human Fas ligand. *J. Exp. Med. 182*, 1777–1783.
6. Mariani, S. M., Matiba, B., Bäumler, C., and Krammer, P. H. (1995) Regulation of cell surface APO-1/Fas (CD95) ligand expression by metalloproteases. *Eur. J. Immunol. 25*, 2303–2307.
7. Martinez-Lorenzo, M. J., Alava, M. A., Anel, A., Piñeiro, A., and Naval, J. (1996) Release of preformed Fas ligand in soluble form is the major factor for activation-induced death of Jurkat T cells. *Immunology 89*, 511–517.
8. Jones, E. Y., Stuart, D. I., and Walker, N. P. C. (1989) Structure of tumour necrosis factor. *Nature 338*, 225–228.
9. Eck, M. J., Ultsch, M., Rinderknecht, E., de Vos, A. M., and Sprang, S. R. (1992) The structure of human lymphotoxin (tumor necrosis factor-beta) at 1.9-Å resolution. *J. Biol. Chem. 267*, 2119–2122.
10. Karpusas, M., Hsu, Y.-M., Wang, J.-H., Thompson, J., Lederman, S., Chess, L., and Thomas, D. (1995) A crystal structure of an extracellular fragment of human CD40 ligand. *Structure 3*, 1031–1039.
11. Schneider, P., Bodmer, J. L., Holler, N., Mattman, C., Scuderi, P., Terkish, A., Peitsch, M. C., and Tschopp, J. (1997) Characterization of Fas (Apo-1, CD95)-Fas ligand interaction. *J. Biol. Chem. 272*, 18827–18833.
12. Krammer, P. H. (2000) CD95's deadly mission in the immune system. *Nature 407*, 789–795.
13. Hohlbaum, A. M., Gregory, M. S., Ju, S. T., and Marshak-Rothstein, A. (2007) Fas ligand engagement of resident peritoneal macrophages in vivo induces apoptosis and the production of neutrophil chemotactic factors. *J. Immunol. 167*, 6217–6224.
14. Straus, S. E., Sneller, M., Lenardo, M. J., Puck, J. M., and Strober, W. (1999) An inherited disorder of lymphocyte apoptosis: the autoimmune lymphoproliferative syndrome. *Ann. Intern. Med. 130*, 591–601.
15. Gruss, H.-J., and Dower, S. (1995) Tumor necrosis factor ligand superfamily: Involvement in the pathology of malignant lymphoma. *Blood 85*, 3378–3404.

16. Sato, K., Kimura, F., Nakamura, Y., Murakami, H., Yoshida, M., Tanaka, M., Nagata, S., Kanatani, Y., Wakimoto, N., Nagata, N., and Motoyoshi, K. (1996) An aggressive nasal lymphoma accompanied by high levels of soluble Fas ligand. *Br. J. Haematol. 94*, 379–382.
17. Oconnell, J., Osullivan, G. C., Collins, J. K., and Shanahan, F. (1996) The Fas counterattack: Fas-mediated T cell killing by colon cancer cells expressing Fas ligand. *J. Exp. Med. 184*, 1075–1082.
18. Strand, S., Hofmann, W. J., Hug, H., Muller, M., Otto, G., Strand, D., Mariani, S. M., Stremmel, W., Krammer, P. H., and Galle, P. R. (1996) Lymphocyte apoptosis induced by CD95 (APO-1/Fas) ligand-expressing tumor cells—A mechanism of immune evasion?. *Nat. Med. 2*, 1361–1366.
19. Hahne, M., Rimoldi, D., Schröter, M., Romero, P., Schreier, M., French, L. E., Schneider, P., Bornand, T., Fontana, A., Lienard, D., Cerottini, J.-C., and Tschopp, J. (1996) Melanoma cell expression of Fas(Apo-1/CD95) ligand: implications for tumor immune escape. *Science 274*, 1363–1366.
20. Westendorp, M. O., Frank, R., Ochsenbauer, C., Stricker, K., Dhein, J., Walczak, H., Debatin, K.-M, and Krammer, P. H. (1995) Sensitization of T cells to CD95-mediated apoptosis by HIV-1 Tat and gp120. *Nature 375*, 497–500.
21. Matute-Bello, G., Liles, W. C., Steinberg, K. P., Kiener, P. A., Mongovin, S, Chi, E. Y., Jonas, M., and Martin, T. R. (1999) Soluble Fas ligand induces epithelial cell apoptosis in humans with acute lung injury (ARDS). *J. Immunol. 163*, 2217–2225.
22. Katsikis, P. D., Wunderlich, E. S., Smith, C. A., Herzenberg, L. A., and Herzenberg, L. A. (1995) Fas antigen stimulation induces marked apoptosis of T lymphocytes in human immunodeficiency virus-infected individuals. *J. Exp. Med. 181*, 2029–2036.
23. Estaquier, J., Tanaka, M., Suda, T., Nagata, S., Golstein, P., and Ameisen, J. C. (1996) Fas-mediated apoptosis of CD4+ and CD8+ T cells from human immunodeficiency virus-infected persons: differential in vitro preventive effect of cytokines and protease antagonists. *Blood 87*, 4959–4966.
24. Dowling, P., Shang, G. F., Raval, S., Menonna, J., Cook, S., and Husar, W. (1996) Involvement of the CD95 (APO-1/Fas) receptor/ligand system in multiple sclerosis brain. *J. Exp. Med. 184*, 1513–1518.
25. Via, C. S., Nguyen, P., Shustov, A., Drappa, J., and Elkon, K. B. (1996) A major role for the Fas pathway in acute graft-versus-host disease. *J. Immunol. 157*, 5387–5393.
26. Braun, M. Y., Lowin, B., French, L., Acha-Orbea, H., and Tschopp, J. (1996) Cytotoxic T cells deficient in both functional Fas ligand and perforin show residual cytolytic activity yet lose their capacity to induce lethal acute graft-versus-host disease. *J. Exp. Med. 183*, 657–661.
27. King, R. D., Saqi, M., Sayle, R., and Sternberg, M. J. (1997) *DSC:* public domain protein secondary structure predication. *Comput. Appl. Biosci. 13*, 473–474.
28. Matute-Bello, G., Liles, W. C., Frevert, C. W., Dhanireddy, S., Ballman, K., Wong, V., Green, R. R., Song, H. Y., Witcher, D. R., Jakubowski, J. A., and Martin, T. R. (2005) Blockade of the Fas/FasL system improves pneumococcal clearance from the lungs without preventing dissemination of bacteria to the spleen. . *Infect. Dis. 191*, 596–606.
29. Wortinger, M. A., Foley, J. W., Larocque, P, Witcher, D. R., Lahn, M., Jakubowski, J. A., Glasebrook, A., and Song, H. Y. (2003) Fas ligand-induced murine pulmonary inflammation is reduced by a stable decoy receptor 3 analogue. *Immunology 110*, 225–233.
30. Demjen, D., Klussmann, S., Kleber, S., Zuliani, C., Stieltjes, B., Metzger, C., Hirt, U. A., Walczak, H., Falk, W., Essig, M., Edler, L., Krammer, P. H., and Martin-Villalba, A. (2004) Neutralization of CD95 ligand promotes regeneration and functional recovery after spinal cord injury. *Nat. Med. 10*, 389–395.
31. Wesche, D. E., Lomas-Neira, J. L., Perl, M., Chung, C. S., and Ayala, A. (2005) Leukocyte apoptosis and its significance in sepsis and shock. *J. Leukocyte Biol. 78*, 325–337.
32. Nakamoto, Y., Kaneko, S, Fan, H., Momoi, T., Tsutsui, H., Nakanishi, K., Kobayashi, K., and Suda, T. (2002) Prevention of hepatocellular carcinoma development associated with chronic hepatitis by anti-fas ligand antibody therapy. *J. Exp. Med. 196*, 1105–1111.
33. Hager-Braun, C., and Tomer, K. B. (2005) Determination of protein derived epitopes by mass spectroscopy. *Expert Rev. Proteomics 2*, 745–756.
34. Englander, S. W. (2006) Hydrogen exchange and mass spectrometry: a historical perspective. *J. Am. Soc. Mass Spectrom. 17*, 1481–1489.
35. Lu, J., Witcher, D. R., White, M. A., Wang, X., Huang, L., Rathnachalam, R., Beals, J. M., and Kuhstoss, S. (2005) IL-1β epitope mapping using site-directed mutagenesis and H/D exchange mass spectrometry analysis. *Biochemistry 44*, 11106–11114.
36. Huber, A., Demartis, S., and Neri, D. (1999) The use of biosensor technology for the engineering of antibodies and enzymes. *J. Mol. Recognit. 12*, 198–216.
37. Schuck, P. (1997) Reliable determination of binding affinity and kinetics using surface plasmon resonance biosensors. *Curr. Opin. Biotechnol. 8*, 498–502.
38. Banner, D. W., D'Arcy, A., Janes, W., Gentz, R., Schoenfeld, H. J., Broger, C., Loetscher, H., and Lesslauer, W. (1993) Crystal structure of the soluble human 55 kd TNF receptor-human TNF beta complex: implications for TNF receptor activation. *Cell 73*, 431–445.
39. Jones, E. Y., Stuart, D. I., and Walker, N. P. (1989) Structure of tumour necrosis factor. *Nature 338*, 225–228.
40. Nisihara, T., Ushio, Y., Higuchi, H., Kayagaki, N., Yamaguchi, N., Soejima, K., Matsuo, S., Maeda, H., Eda, Y., Okumura, K., and Yagita, H. (2001) Humanization and epitope mapping of neutralizing anti-human Fas ligand monoclonal antibodies: structural insights into Fas/Fas ligand interaction. *J. Immunol. 167*, 3266–3275.
41. Starling, G. C., Bajorath, J., Emswiler, J., Ledbetter, J. A., Aruffo, A., and Kiener, P.A. (1997) Identification of amino acid residues important for ligand binding to Fas. *J. Exp. Med. 185*, 1487–1492.